Porphyrins

International Edition: DOI: 10.1002/anie.201601303
German Edition: DOI: 10.1002/ange.201601303

# Synthesis of Di-*peri*-dinaphthoporphyrins by $PtCl_2$-Mediated Cyclization of Quinodimethane-type Porphyrins

*Masataka Umetani, Koji Naoda, Takayuki Tanaka,* Seung-Kyu Lee, Juwon Oh, Dongho Kim,* and Atsuhiro Osuka**

***Abstract:*** *Di-peri-dinaphthoporphyrins can be regarded as a key and common substructure of fused porphyrinoids. $PtCl_2$-mediated cycloisomerization reaction of quinodimethane-type porphyrins provided these doubly fused porphyrins, which exhibit characteristic paratropic ring currents that presumably arise from 24π antiaromatic circuit as a dominant resonance contributor. UV/Vis absorption spectra, cyclic voltammetry, and excited-state dynamics as well as theoretical calculation support this conclusion.*

In recent years fused porphyrinoids have attracted much attention because of their promising properties as NIR-absorbing and emitting dyes, pigments of photodynamic therapy, non-linear optical materials, and electron conducting materials.[1] Among these, *meso–meso*, β–β, β–β triply-linked porphyrin arrays (porphyrin tape **1**, Figure 1) possess a unique position in light of their remarkable bathochromic absorption shifts reaching the infrared region that arise from the effective electronic delocalization over the entire molecule.[2] Various porphyrins fused with other aromatic segments such as anthracene-fused porphyrin **2** and BODIPY-fused porphyrin **3** have been also explored.[3] In these examples, the aromatic characters of the porphyrin segments are mitigated due to the electron delocalization into the fused segments. As notable examples, Wu et al. reported fused quinonoidal porphyrin **4** which exhibits a nonaromatic nature intrinsic to the quinonoidal conjugation as a result of acquiring stabilization due to four Clar's sextet benzenes.[4,5] They also synthesized phenarenyl-fused porphyrin **5** that was an open-shell biradical and was easily oxidized by air to form oxygenated derivatives.[6] In these cases, two or more aromatic units are linked by triple C–C bonds, giving rise to formal naphthalene segments directly attached on the porphyrin peripheries (as emphasized in the structure of **1**). Thus, we naturally became interested in the common interior core, namely di-*peri*-dinaphthoporphyrin, whose nomenclature derives from analogy to hexa-*peri*-hexabenzocoronene. Intriguingly, the conjugation circuit

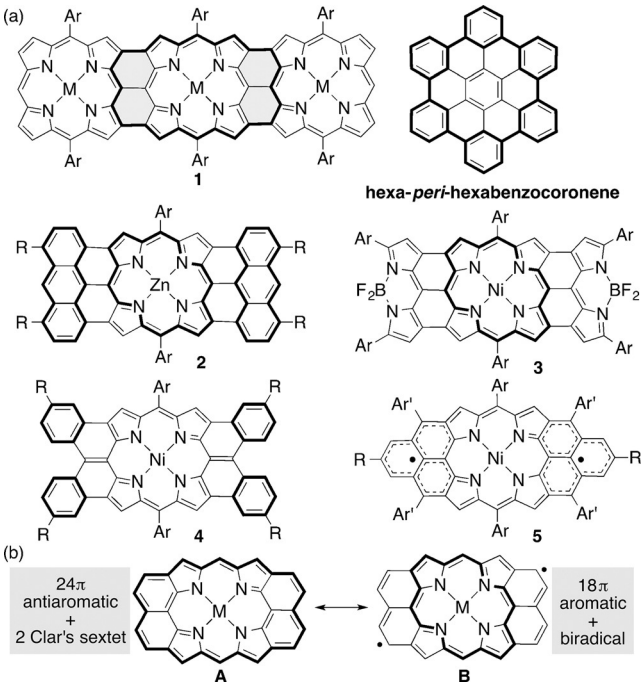


***Figure 1.*** a) Porphyrin tape **1**, hexa-*peri*-hexabenzocoronene, and precedent fused porphyrinoids **2**–**5**. b) Resonance structures of di-*peri*-dinaphthoporphyrin between **A** (closed-shell: 24π antiaromatic circuit with two Clar's sextets) and **B** (biradical: 18π aromatic circuit).

of this unique fused porphyrin cannot be simply delineated as the usual porphyrin 18π circuit. As shown in Figure 1b, resonance form **A** represents a closed-shell 24π-antiaromatic circuit together with two Clar's sextet benzenes and resonance form **B** is delineated as a biradical with a 18π-aromatic porphyrin network. These two forms may be competitive to determine the actual electronic state. Herein we report the synthesis of *peri*-naphtho-fused porphyrin **10** and its electronic properties.

First, 5,15-dioxoporphodimethene **6H**[4,7] was transformed to tetrabromide **7H** by Corey–Fuchs reaction with tetrabromomethane in the presence of triphenylphosphine, which was then metalated with $Ni^{II}(acac)_2$ to give $Ni^{II}$ complex **7Ni** (Scheme 1). Quinodimethane-type porphyrin **8Ni** was synthesized by Stille coupling of **7Ni** with 8 equiv of tributyl(phenylethynyl)tin in 59% yield. Reaction of **8Ni** with 0.6 equiv of $PtCl_2$ afforded a 2-fold cyclization product **9Ni** in 21% yield.[8,9] When the reaction was conducted with 2 equiv of $PtCl_2$ in toluene at 90 °C, the formation of a 4-fold cyclization product **10Ni** was observed in a small amount along with many side products. We could not isolate **10Ni** in

[*] M. Umetani, K. Naoda, Dr. T. Tanaka, Prof. Dr. A. Osuka
Department of Chemistry, Graduate School of Science, Kyoto University
Sakyo-ku, Kyoto 606-8502 (Japan)
E-mail: osuka@kuchem.kyoto-u.ac.jp
S.-K. Lee, J. Oh, Prof. Dr. D. Kim
Spectroscopy Laboratory for Functional π-Electronic Systems and Department of Chemistry, Yonsei University
Seoul 120-749 (Korea)
E-mail: dongho@yonsei.ac.kr

Supporting information for this article can be found under: http://dx.doi.org/10.1002/anie.201601303.

  

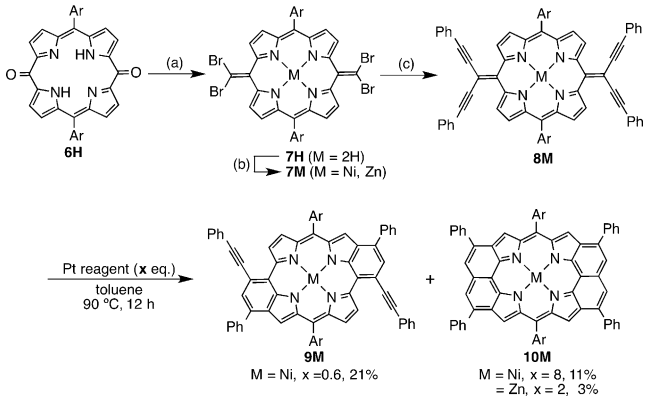


***Scheme 1.*** Synthesis of di-*peri*-dinaphthoporphyrins **10M**. Reagents and conditions; a) $CBr_4$, $PPh_3$, toluene, 80 °C, 12 h, 75%; b) M = Ni: Ni(acac)$_2$, toluene, reflux, 3 h, 91%, M = Zn: Zn(OAc)$_2$·2 $H_2O$, $CH_2Cl_2$, MeOH, RT, 1 h, 91%; c) tributyl(phenylethynyl)tin, $Pd_2(dba)_3$, P(2-furyl)$_3$, toluene, 80 °C, 1 h, 59% (M = Ni), 38% (M = Zn). Ar = 3,5-di-*tert*-butylphenyl.

a pure form from this reaction mixture. After screening of various platinum salts, we found that use of 8 equiv of $Pt(MeCN)_2Cl_2$ resulted in a cleaner reaction that allowed for the isolation of **10Ni** in 11% yield. The structures of **8Ni**, **9Ni**, and **10Ni** were confirmed by X-ray diffraction analysis (Figure 2).[10] Compounds **8Ni** and **9Ni** show gable-like bent structures with mean-plane deviation (MPD) values of 0.49 and 0.32 Å, respectively.[11] These bent structures are considered to arise from the steric repulsion between the β-protons and phenylethynyl groups. In contrast, the structure of **10Ni** has been shown to be quite planar with an MPD value of only 0.050 Å. The C=C double bond length of the *exo* methylene group is 1.38 Å in **8Ni**, indicating its typical double bond character, while those of **9Ni** and **10Ni** are both 1.41 Å, respectively. The newly formed benzene rings of **9Ni** and **10Ni** do not display significant bond-length alterations and the HOMA values of these benzene rings are calculated to be 0.71 and 0.83, respectively.[12] Interestingly, among several possible 2-fold cyclized products, only **9Ni** was selectively formed probably due to structural restriction or electronic reason in the preformed 1-fold cyclized product (See Figure S8-3 in the Supporting Information, SI).

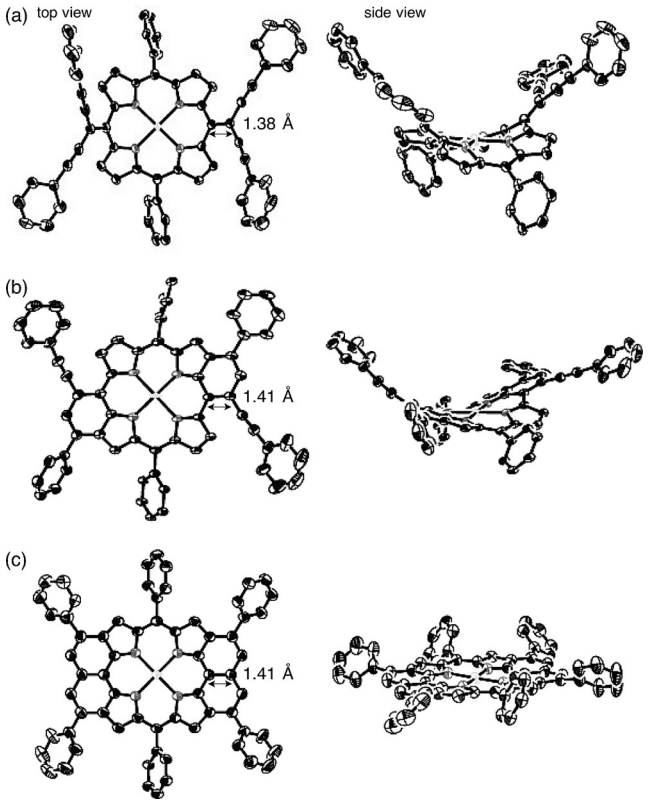


***Figure 2.*** X-ray crystal structures of a) **8Ni**, b) **9Ni**, and c) **10Ni**. *tert*-Butyl groups, solvent molecules, and hydrogen atoms are omitted for clarity. The thermal ellipsoids are scaled to the 50% probability.

The $^1$H NMR spectrum of **8Ni** showed two doublets at 7.35 and 6.67 ppm due to the β-protons, and that of **9Ni** exhibited three signals due to the β-protons at 8.16, 7.34, and 7.20 ppm and a singlet at 6.92 ppm due to the *peri*-benzene protons (SI). These chemical shifts are consistent with their nonaromatic characters as confirmed by comparison with the $^1$H NMR spectrum of aromatic **11Ni**. On the other hand, $^1$H NMR spectrum of **10Ni** showed two singlets at 5.64 and 5.23 ppm due to the β-protons and naphthalene protons, respectively, which are certainly upfield shifted as compared with those of **8Ni** and **9Ni**, indicating a distinct paratropic ring current.

In the next step, we attempted to obtain freebase **10H** by demetalation of **10Ni** under various conditions, but failed to find suitable reaction conditions. We thus decided to synthesize **10Zn** as a precursor of **10H**. $Zn^{II}$ complex **7Zn** was prepared by zincation of **7H** and was converted to **8Zn** by Stille coupling. Cyclization of **8Zn** was conducted under similar conditions used for the synthesis of **10Ni**, giving **10Zn** in 3% yield.[13] Treatment of **10Zn** with aqueous HCl gave **10H** in good yield. The $^1$H NMR spectrum of **10H** showed a signal at 18.42 ppm due to the inner NH protons, and two singlets at 6.05 and 5.94 ppm due to the β-protons and naphthalene protons, respectively, indicating its distinct paratropic ring-current effect. Fortunately, single crystals were obtained from a solution of **10H** in THF and methanol (Figure 3a).[10] Similarly to **10Ni**, freebase **10H** displays a planar structure with an MPD value of 0.050 Å. The HOMA values of four benzene rings fused on the *peri*-region are 0.76 and 0.63, indicating slightly clearer bond-length alternation. The $^1$H NMR signals of its outer-protons (6.05 and 5.94 ppm) are slightly downfield shifted as compared with those of **10Ni** and **10Zn** probably due to a weaker paratropic ring-current effect. The antiaromatic natures of **10H**, **10Zn** and **10Ni** are evaluated by nucleus-independent chemical shift (NICS) and anisotropy of induced current density (AICD) calculations (Figures 2 and S8-4–6 in SI).[14,15] The calculated NICS values of **10H**, **10Zn**, and **10Ni** are all positive inside the tetrapyrrole macrocycles, and the NICS value at the center of **10H** is + 7.75 ppm. These positive NICS values indicate the antiaromatic characters of **10H**, **10Zn** and **10Ni**. The AICD plot of **10H** shows a counter-clockwise current flow that involves *peri*-benzene regions. Thus, the observed paratropic ring current can be ascribed to 24π antiaromatic circuit with the aid of the Clar's sextet effect.[16]

  

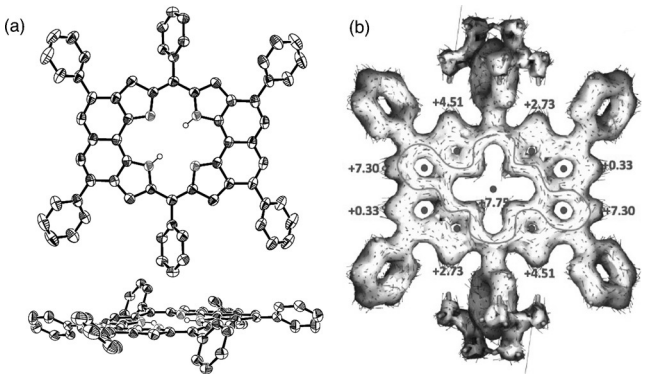


***Figure 3.*** a) X-ray crystal structure of **10H**. *tert*-Butyl groups, solvent molecules, and hydrogen atoms except for NHs are omitted for clarity. The thermal ellipsoids are scaled to the 50% probability. b) AICD plot for **10H** (isosurface value: 0.03). The NICS(0) values at the central points of constitutional rings are also shown.

Despite the antiaromatic characters, **10Ni** and **10Zn** are stable compounds and can be stored as solids without deterioration under ambient conditions over several months.

The UV/Vis absorption spectra of **8Ni**, **9Ni**, **10Ni**, and **11Ni** in $CH_2Cl_2$ are shown in Figure 4a. $Ni^{II}$ porphyrin **11Ni** exhibits a sharp Soret band at 401 nm and a weak Q band at 516 nm. Compared to **11Ni**, compounds **8Ni** and **9Ni** display weak, broad and ill-defined absorption spectra with low-energy absorption bands at 734 and 790 nm, respectively, indicating that their porphyrinic π-electron systems are largely perturbed by peripheral groups. On the other hand, **10Ni** exhibits a sharp Soret-like band at 522 nm and a red-shifted band at 897 nm with very weak absorption tail reaching to around 1300 nm. The similar spectral features were observed for **10Zn** and **10H** (Figure 4b). These weak absorption tails refer to the presence of NIR dark states, which is a characteristic feature of antiaromatic porphyrinoids.[17,18]

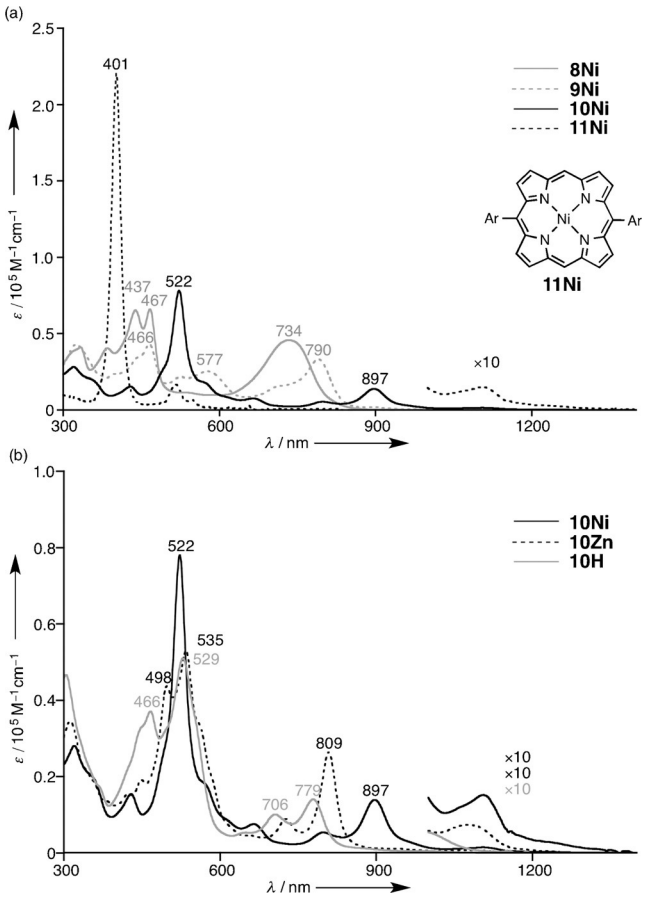


***Figure 4.*** UV/Vis/NIR absorption spectra of a) **8Ni**, **9Ni**, **10Ni**, and **11Ni**, b) **10Ni**, **10Zn**, and **10H** in $CH_2Cl_2$.

Femtosecond transient absorption (TA) measurements were carried out for **8Ni** and **10Ni**. (Figure S10). **8Ni** exhibits a double exponential decay profile (12 and 800 ps) without fluorescence emission. This excited state dynamics of **8Ni** can be explained by $Ni^{II}$-centered (d,d) state of typical $Ni^{II}$ porphyrinoids, where the excited population undergoes a rapid internal conversion (IC) process to the (d,d) state and subsequent deactivation process to the ground state on the order of hundreds ps.[19] On the other hand, the TA absorbance of **10Ni** decays rapidly with two time constants of 1.2 and 12 ps. The ultrafast relaxation dynamics can be comprehended by the optically dark state, characteristic of antiaromatic porphyrinoids.[16] Since the dark state acts as a ladder in the deactivation process to the ground state, **10Ni** shows fast IC process to the dark state with $\tau = 1.2$ ps and subsequent relaxation to the ground state with $\tau = 12$ ps. Two-photon absorption (TPA) measurements were carried out for **8Ni** and **10Ni** by using an open-aperture Z-scan method in the range of 1200–1900 nm, whereby one-photon absorption is negligible. The TPA cross-section values are 190 GM for **8Ni** at 1400 nm, and 380 GM for **10Ni** at 1800 nm, respectively (Figures S11-1, S11-2). The observed larger TPA value of **10Ni** can be ascribed to the reduced HOMO–LUMO gap arising from extended π-conjugation.[20]

Cyclic voltammetry and differential-pulse voltammetry (DPV) experiments have been conducted in $CH_2Cl_2$ against ferrocene/ferrocenium ion couple (Table 1). These experiments exhibited two reduction potentials at −1.10 and −1.49 V for **8Ni** and at −1.13 and −1.58 V for **9Ni**, and one oxidation potential at 0.32 V for **8Ni** and at 0.34 V for **9Ni**. The electrochemical HOMO–LUMO gaps ($\Delta E_{HL}$) are determined to be 1.42 and 1.47 eV for **8Ni** and **9Ni**, respectively. **10Ni** exhibited two reversible reduction waves at −0.92 and −1.48 V and three reversible oxidation waves at 0.31, 0.38,

***Table 1:*** Electrochemical properties of **8Ni**, **9Ni**, **10Ni**, **10Zn**, and **10H** measured in $CH_2Cl_2$.[a]

| Compd. | $E_{ox.3}$ | $E_{ox.2}$ | $E_{ox.1}$ | $E_{red.1}$ | $E_{red.2}$ | $\Delta E_{HL}$[c] |
|---|---|---|---|---|---|---|
| **8Ni** | – | – | 0.32[b] | −1.10 | −1.49 | 1.42 |
| **9Ni** | – | – | 0.34[b] | −1.13 | −1.58 | 1.47 |
| **10Ni** | 0.80 | 0.38 | 0.31 | −0.92 | −1.48 | 1.23 |
| **10Zn** | – | 0.70 | 0.29 | −1.01 | −1.53 | 1.30 |
| **10H** | – | – | 0.45 | −0.95 | −1.43 | 1.40 |

[a] Potentials [V] vs. ferrocene/ferrocenium ion. Scan rate 0.05 $Vs^{-1}$; working electrode, glassy carbon; counter electrode, Pt wire; supporting electrolyte, 0.1 M $nBu_4NPF_6$; reference electrode, $Ag/AgClO_4$. [b] Irreversible peaks. [c] Electrochemical HOMO–LUMO gaps ($\Delta E_{HL} = E_{ox.1} - E_{red.1}$ [eV]).

  

and 0.80 V. The first reduction potential of **10Ni** is anodically shifted from those of **8Ni** and **9Ni** and thus the electrochemical HOMO–LUMO gap of **10Ni** is decreased ($\Delta E_{HL} = 1.23$ eV). The first oxidation potential of **10H** is higher than that of **10Ni**, which leads to a larger $\Delta E_{HL}$ value (1.40 eV). These results are roughly consistent with those obtained by DFT calculations (Figure S8-1). It is worthy to note that the LUMO energy levels of **10M** are lower than those of dimeric porphyrin tapes,[2a–d] while the HOMO levels remain intact. Indeed, addition of an equimolar amount of cobaltocene to a solution of **10Ni** in THF caused a clean change to its radical anion with NIR absorption bands at 1137, 1194, and 1402 nm via clear isosbectic points (Figure S9-2). The reduced species was ESR active, displaying a sharp signal with $g = 2.0026$ (Figure S9-3). In addition, chemical oxidation of **10Ni** proceeded in a stepwise manner upon treatment with tris(*p*-bromophenyl)aminium hexachloroantimonate (Figure S9-1). Such an ambipolar character of di-*peri*-dinaphthoporphyrin is promising an application for multi-charge storage materials[2c] and organic rechargeable batteries.[21]

In summary, we have synthesized di-*peri*-dinaphthoporphyrin **10M** via $PtCl_2$-mediated cycloisomerization reaction of quinodimethane-type porphyrins. The $^1$H NMR, UV/Vis absorption spectra, cyclic voltammetry, and theoretical calculation of **10M** supported the presence of 24π antiaromatic contribution. The freebase **10H** displayed a weak paratropic ring-current effect. The observed smaller HOMO–LUMO gaps of **10M** arise from stabilized LUMO levels. These characteristic properties provide an important clue to understand the intrinsic physical properties of the fused porphyrinoids.

## Acknowledgements

The work at Kyoto was supported by JSPS KAKENHI (Grant Numbers 26810021, 25220802 and 25620031). K.N. acknowledges a JSPS Fellowship for Young Scientists. The work at Yonsei University was supported by Global Research Laboratory (2013K1A1A2A02050183) through the National Research Foundation of Korea (NRF) funded by the Ministry of Science, ICT (Information and Communication Technologies) and Future Planning. The authors thank Dr. Takahisa Ikeue (Shimane University) for the ESR measurement.

**Keywords:** antiaromaticity · cyclic voltammetry · cycloisomerization · porphyrin · porphyrin tape

**How to cite:** *Angew. Chem. Int. Ed.* **2016**, *55*, 6305–6309
*Angew. Chem.* **2016**, *128*, 6413–6417

[1] a) J. R. Reimers, N. S. Hush, M. J. Crossley, *J. Porphyrins Phthalocyanines* **2002**, *6*, 795; b) S. Fox, R. W. Boyle, *Tetrahedron* **2006**, *62*, 10039; c) N. Aratani, D. Kim, A. Osuka, *Chem. Asian J.* **2009**, *4*, 1172; d) C. Jiao, J. Wu, *Synlett* **2012**, 171; e) J. P. Lewtak, D. T. Gryko, *Chem. Commun.* **2012**, *48*, 10069; f) A. M. V. M. Pereiraa, S. Richetera, C. Jeandona, J.-P. Gisselbrechta, J. Wytkoa, R. Ruppert, *J. Porphyrins Phthalocyanines* **2012**, *16*, 464; g) H. Mori, T. Tanaka, A. Osuka, *J. Mater. Chem. C* **2013**, *1*, 2500; h) T. Tanaka, A. Osuka, *Chem. Soc. Rev.* **2015**, *44*, 943.

[2] a) A. Tsuda, H. Furuta, A. Osuka, *Angew. Chem. Int. Ed.* **2000**, *39*, 2549; *Angew. Chem.* **2000**, *112*, 2649; b) A. Tsuda, A. Osuka, *Science* **2001**, *293*, 79; c) D. Bonifazi, M. Scholl, F. Song, L. Echegoyen, G. Accorsi, N. Armaroli, F. Diederich, *Angew. Chem. Int. Ed.* **2003**, *42*, 4966; *Angew. Chem.* **2003**, *115*, 5116; d) T. Ikeda, N. Aratani, A. Osuka, *Chem. Asian J.* **2009**, *4*, 1248.

[3] a) N. K. S. Davis, A. L. Thompson, H. L. Anderson, *Org. Lett.* **2010**, *12*, 2124; b) N. K. S. Davis, A. L. Thompson, H. L. Anderson, *J. Am. Chem. Soc.* **2011**, *133*, 30; c) C. Jiao, L. Zhu, J. Wu, *Chem. Eur. J.* **2011**, *17*, 6610.

[4] W. Zeng, B. S. Lee, Y. M. Sung, K.-W. Huang, Y. Li, D. Kim, J. Wu, *Chem. Commun.* **2012**, *48*, 7684.

[5] a) E. Clar, *Polycyclic Hydrocarbons*, Academic Press, London, **1964**; b) M. Randic, *Chem. Rev.* **2003**, *103*, 3449.

[6] W. Zeng, S. Lee, M. Son, M. Ishida, K. Furukawa, P. Hu, Z. Sun, D. Kim, J. Wu, *Chem. Sci.* **2015**, *6*, 2427.

[7] a) D. Lahaye, K. Muthukumaran, C.-H. Hung, D. Gryko, J. S. Rebouças, I. Spasojević, I. Batinić-Haberle, J. S. Lindsey, *Bioorg. Med. Chem.* **2007**, *15*, 7066; b) N. L. Bill, M. Ishida, S. Bähring, J. M. Lim, S. Lee, C. M. Davis, V. M. Lynch, K. A. Nielsen, J. O. Jeppesen, K. Ohkubo, S. Fukuzumi, D. Kim, J. L. Sessler, *J. Am. Chem. Soc.* **2013**, *135*, 10852.

[8] a) D. P. Arnold, R. G. Holmes, A. W. Johnson, A. R. P. Smith, G. A. Williams, *J. Chem. Soc. Perkin Trans. 1* **1978**, 1660; b) M. G. H. Vicente, I. N. Rezzano, K. M. Smith, *Tetrahedron Lett.* **1990**, *31*, 1365; c) M. G. H. Vicente, K. M. Smith, *J. Org. Chem.* **1991**, *56*, 4407; d) A. R. Morgan, S. Gupta, *Tetrahedron Lett.* **1994**, *35*, 5347.

[9] L. J. K. Boerner, D. F. Dye, T. Köpke, J. M. Zaleski, *Coord. Chem. Rev.* **2013**, *257*, 599.

[10] Crystallographic data for **8Ni**; $C_{82}H_{70}N_4Ni$, $0.53\,(CH_2Cl_2)$; $M_w = 1215.13\,g\,mol^{-1}$; monoclinic; *P* 2/*n* (No.13); $a = 21.287(5)$, $b = 11.687(2)$, $c = 28.514(6)$ Å; $\beta = 111.753(5)°$; $V = 6589(2)$ Å$^3$; $Z = 4$; $\rho_{calcd} = 1.225\,g\,cm^{-3}$; $R1 = 0.1086$ [$I > 2\sigma(I)$]; $wR2 = 0.3151$ (all data); GOF = 1.073; Crystallographic data for **9Ni**; $C_{82}H_{70}N_4Ni$, $2\,(C_6H_5Cl)$; $M_w = 1395.21\,g\,mol^{-1}$; triclinic; $P\bar{1}$ (No. 2); $a = 14.9249(11)$, $b = 15.6008(10)$, $c = 16.9809(14)$ Å; $\alpha = 73.799(18)$, $\beta = 75.88(2)$, $\gamma = 72.151(18)°$; $V = 3559.4(7)$ Å$^3$; $Z = 2$; $\rho_{calcd} = 1.302\,g\,cm^{-3}$; $R1 = 0.0704$ [$I > 2\sigma(I)$]; $wR2 = 0.2153$ (all data); GOF = 1.011; Crystallographic data for **10Ni**; $C_{82}H_{68.57}N_4Ni$, $2\,(C_7H_8)$, $0.35\,(CO)$; $M_w = 1362.74\,g\,mol^{-1}$; monoclinic; *P*21/*c* (No.14); $a = 20.126(6)$, $b = 18.285(5)$, $c = 20.711(6)$ Å; $\beta = 101.835(9)°$; $V = 7460(4)$ Å$^3$; $Z = 4$; $\rho_{calcd} = 1.213\,g\,cm^{-3}$; $R1 = 0.0860$ [$I > 2\sigma(I)$]; $wR2 = 0.2825$ (all data); GOF = 1.004; Crystallographic data for **10H**; $C_{82}H_{72}N_4Ni$, $(C_4O)$; $M_w = 1177.48\,g\,mol^{-1}$; monoclinic; *C*2/*c* (No.15); $a = 25.625(7)$, $b = 18.524(5)$, $c = 14.530(4)$ Å; $\beta = 111.845(7)°$; $V = 6402(3)$ Å$^3$; $Z = 4$; $\rho_{calcd} = 1.222\,g\,cm^{-3}$; $R1 = 0.0516$ [$I > 2\sigma(I)$]; $wR2 = 0.1655$ (all data); GOF = 1.040; CCDC 1451282, 1451281, and 1451280 contain the supplementary crystallographic data for this paper. These data can be obtained free of charge from The Cambridge Crystallographic Data Centre.

[11] The mean-plane deviations of **8Ni**, **9Ni** and **10Ni** were defined by core 24 atoms of porphyrin unit.

[12] a) T. M. Krygowski, T. M. Cryański, *Tetrahedron* **1996**, *52*, 1713; b) T. M. Krygowski, T. M. Cryański, *Tetrahedron* **1996**, *52*, 10255.

[13] We thought that particular instabilities of **8Ni** and **8Zn** are a main reason for the low yields of **10Ni** and **10Zn**. We did not observe the formation of meaningful side products in the cyclization reactions of **8Ni** and **8Zn**.

[14] a) P. v. R. Schleyer, C. Maerker, A. Dransfeld, H. Jiao, N. J. R. van Eikema Hommes, *J. Am. Chem. Soc.* **1996**, *118*, 6317; b) Z. Chen, C. S. Wannere, C. Corminboeuf, R. Puchta, P. v. R. Schleyer, *Chem. Rev.* **2005**, *105*, 3842.

  

[15] a) D. Geuenich, K. Hess, F. Köhler, R. Herges, *Chem. Rev.* **2005**, *105*, 3758; b) R. Herges, D. Geuenich, *J. Phys. Chem. A* **2001**, *105*, 3214; c) R. Herges, *Chem. Rev.* **2006**, *106*, 4820.

[16] As described in the introduction part in the text, compounds **1**, **2**, and **3** are all aromatic but their aromatic characters are mitigated due to the fused structures. Consistent with the relatively small electronic perturbations, the porphyrin electronic networks of **1**, **2**, and **3** can be delineated as shown in Figure 1. But such delineation is difficult for porphyrins **4**, **5**, and **10M**. The four peripheral benzene rings in **4** maintain the local aromaticity, hence decreasing the contribution of the peripheral antiaromatic macrocyclic network. The fusion of the phenalenyl segments (a typical radical segment) leads to an open shell molecule **5**. Porphyrins **10M** possess the bare di-*peri*-naphthoporphyrin chromophore, in which the outside peripheral electronic network is effective, allowing the antiaromatic character.

[17] a) M.-C. Yoon, S. Cho, M. Suzuki, A. Osuka, D. Kim, *J. Am. Chem. Soc.* **2009**, *131*, 7360; b) J. M. Lim, Z. S. Yoon, J.-Y. Shin, K. S. Kim, M.-C. Yoon, D. Kim, *Chem. Commun.* **2009**, 261; c) S. Cho, Z. S. Yoon, K. S. Kim, M. C. Yoon, D. G. Cho, J. L. Sessler, D. Kim, *J. Phys. Chem. Lett.* **2010**, *1*, 895.

[18] Phenanthriporphyrin has been recently reported by L. Latos-Grażyński et al., which displays an antiaromatic character; B. Szyszko, A. Białońska, L. Szterenberg, L. Latos-Grażyński, *Angew. Chem. Int. Ed.* **2015**, *54*, 4932; *Angew. Chem.* **2015**, *127*, 5014.

[19] a) T. C. Gunaratne, A. V. Gusev, X. Peng, A. Rosa, G. Ricciardi, E. J. Baerends, C. Rizzoli, M. E. Kenney, M. A. J. Rodgers, *J. Phys. Chem. A* **2005**, *109*, 2078; b) D. Rais, P. Toman, J. Černý, M. Menšík, J. Pfleger, *J. Phys. Chem. A* **2014**, *118*, 5419; c) X. Zhang, E. C. Wasinger, A. Z. Muresan, K. Attenkofer, G. Jennings, J. S. Lindsey, L. X. Chen, *J. Phys. Chem. A* **2007**, *111*, 11736; d) J. Oh, H. Yoon, Y. M. Sung, P. Kang, M.-G. Choi, W.-D. Jang, D. Kim, *J. Phys. Chem. B* **2015**, *119*, 7053.

[20] a) K. Kurotobi, K. S. Kim, S. B. Noh, D. Kim, A. Osuka, *Angew. Chem. Int. Ed.* **2006**, *45*, 3944; *Angew. Chem.* **2006**, *118*, 4048; b) P. Kim, S. Ham, J. Oh, H. Uoyama, H. Watanabe, K. Tagawa, H. Uno, D. Kim, *Phys. Chem. Chem. Phys.* **2013**, *15*, 10612.

[21] J.-Y. Shin, T. Yamada, H. Yoshikawa, K. Awaga, H. Shinokubo, *Angew. Chem. Int. Ed.* **2014**, *53*, 3096; *Angew. Chem.* **2014**, *126*, 3160.

Received: February 4, 2016
Revised: March 21, 2016
Published online: April 13, 2016

  